FAST AND EFFECTIVE CHARACTERIZATION OF 3D REGION DATA

Vasileios Megalooikonomou, Haimonti Dutta, Despina Kontos

Department of Computer and Information Sciences, Temple University, Philadelphia, PA, USA

ABSTRACT

We consider the problem of characterization of spatial region data such as the regions of interest (ROIs) in medical images. We propose a method that efficiently extracts a k-dimensional feature vector using concentric spheres in 3D (or circles in 2D) radiating out of the ROI's center of mass. The proposed method can be applied to classification and similarity searches of ROIs. We also propose a region data growth model that we use to generate artificial data with various properties including homogeneous and non-homogeneous region data. We use the artificial data to evaluate the effectiveness of the characterization method comparing also its classification performance to mathematical morphology. The experiments show that the performance of our method is comparable or better than that of mathematical morphology although it is two orders of magnitude faster which makes it very suitable for application in very large image databases.

1. INTRODUCTION

Analysis of images usually refers to the extraction of their information content. Methods for content-based retrieval and classification of images rely on effective and efficient techniques for the extraction of the most important and discriminative features [1]. Most of the characterization techniques are based on extracted features that refer to the entire image [2,3] rather than to image regions that are of interest. However, analysis of images in certain fields such as medicine require focusing on specific Regions of Interest (ROI's), such as tumors, lesions and brain activation regions, in order to analyze critical information [4-6]. The 3D volumes (or 2D images) we consider here consist of region data that can be defined as sets of (often connected) voxels (volume elements) that form structures or objects. In this paper we propose a method to quantitatively characterize spatial region data visualized by modern imaging modalities, such as MRI (Magnetic Resonance Imaging) and CT (Computed Tomography). Furthermore, we evaluate its effectiveness by examining the Euclidean distances of the characterizing vectors for several types of regions and we compare our method with mathematical morphology.

2. BACKGROUND AND RELATED WORK

Representing a shape corresponding to a certain ROI has been the main issue of various attempts to characterize spatial data [7,8]. Necessary preprocessing steps for the characterization and classification of ROIs are the segmentation and registration of the corresponding images. Image segmentation is required to delineate the particular regions that are of interest while image registration is required to bring the images into spatial coincidence with a template and it is also referred to as spatial normalization. Throughout the paper we assume that the region data are segmented and registered.

Shape is the geometrical information that remains when location, scale and rotational effects are filtered out from an object [9]. Shape representation and analysis has generated a rich array of approaches from simpler ones that use anatomical or mathematical landmarks, simpler shapes and polygonalization to more advanced ones that extend to obtaining numerical vectors from various transforms of the boundary, such the Fourier Transform, Wavelet Transform or moments of inertia. Concepts from mathematical morphology, namely the "pattern spectrum" of a shape, have also been used to map a shape to a point in a *k*-dimensional space [10] effectively characterizing and classifying it [11]. Mappings are defined in terms of a structural element, a "small" primitive shape that interacts with the input image (via morphological operators like dilation, erosion, opening (○), and closing (●)) to transform it and in the process, extract useful information about its geometrical and topological structure [12].

The morphological distance between two objects x_1 and x_2 is defined as:

$$d^E_{morph}(x_1, x_2) = \left(\sum_{m=-M}^{M} \left| d^*(f^E_m(x_1), f^E_m(x_2)) \right|^p \right)^{1/p}$$

with

$$f^E_m(x) = \begin{cases} x \circ mE, & 1 \le m < M \\ x, & m = 0 \\ x \bullet mE, & -M \le m \le -1 \end{cases}$$

where E is some structuring element, d^* is the area of the symmetric set difference distance measure defined as $d^*(x_1, x_2) = |x_1 \cup x_2| - |x_1 \cap x_2|$ after the objects have been optimally aligned via registration, and p denotes the particular norm used (e.g., p=2, for Euclidean distance).

Most of the techniques for shape characterization work mostly with homogeneous objects (i.e., binary images) without considering properties of the internal volume and are computationally expensive especially when they are applied to 3D volumes. In this paper we propose a new characterization technique that performs very well for both homogeneous and non-homogeneous regions and is much faster than existing techniques making it suitable for approximate searches of similar regions in large image databases.

3. METHODOLOGY

In order to characterize ROIs we extend the original idea of Sholl's analysis [13] (i.e. the use of concentric circles radiating out of the root of the tree to partition a tree-like structure) to non-tree like structures in order to obtain a characterization vector of k attributes mapping a ROI to a point in the k-dimensional space. Classification and similarity searches can then be achieved using the corresponding vectors that quantitatively characterize the structure. Although the characterization of ROIs is of particular interest in medical image databases [5], the methodology we propose can be applied to non-medical image data as well.

3.1. Characterization of ROIs

In this paper we deal with the characterization of two different types of regions: (a) homogeneous, where all the voxels that form the regions have the same value which is different from the background (binary images) and (b) non-homogeneous, where the values of voxels that form the regions can range while they are still different from the background (non-binary or gray scale images). Figure 1 shows examples of homogeneous and non-homogeneous regions. Another way to view non-homogeneous regions is that the voxel values reflect a probability that the voxels belong to a ROI as in the case of uncertainty in delineating the boundaries of certain structures in medical images or in the case of statistical parametric maps obtained from analysis of fMRI (functional Magnetic Resonance Imaging) activations.

The basic problem we are considering here is the following: Given a homogeneous or non-homogeneous ROI, effectively extract useful features, so that characterization, classification and retrieval of similar structures can be performed efficiently. The proposed method for characterization is the following:

1. Obtain the center of mass of the region. Note that in the case of non-homogeneous regions the center of mass is calculated using a weighted contribution of each voxel of the region, based on each value.
2. Using the center of mass as center, construct a series of 1…k concentric spheres in 3D (or circles in 2D) with regular increments of their radius.
3. For each sphere (or circle) measure features such as (a) the fraction of the sphere (or circle) occupied by the region, (b) the fraction of the region occupied by the sphere (circle), forming respectively feature vectors f_s and f_r of size k.

Experimental results illustrate the comparative effectiveness of both types of features in step 3 above. Figure 2 shows the process of characterization by capturing snapshots of the intersection of the concentric spheres and a 3D ROI that is being analyzed. The obtained vector maps the entire ROI to a specific point in the k-dimensional space. Classification and similarity searches can be performed using geometrical distance measurements between the corresponding vectors, or other classification models such as Neural Networks. We propose the use of dimensionality reduction techniques, such as the Karhunen-Loève transform or the closely related Singular Value Decomposition (SVD), for projecting the characterization vector to a lower dimensionality space. In addition, for a given training set and classes of ROIs, experimentation can be done as a part of this approach to obtain an appropriate value for the increment of radius of the concentric sphere in each step so that an optimal classification performance is achieved.

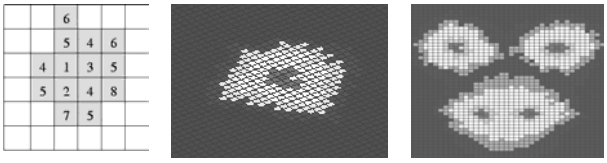

(a) (b) (c)

Figure 1. (a) A homogeneous region (the cell infection is shown at time t=8 in a 2D grid), (b),(c) non-homogeneous regions with one and three initial points respectively.

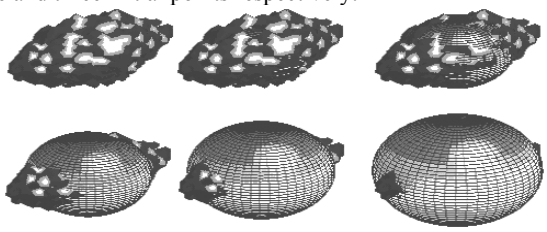

Figure 2. Intersecting concentric spheres with the ROI being characterized.

3.2. Generation of artificial regions

We developed a discrete-time region growth model based on the 2-D model originally proposed by Eden [14] and which has been used in studies of similarity searches [11]. The main idea of this model and sample ROIs in 2-D are presented in Figure 1. The growth (infection) process begins with one initial voxel (or cell) at time t=0 and progresses using the following rule: each infected cell may infect its non-diagonal neighbors with some probability. We have extended this model by allowing the probability thresholds to be different for each direction. For example, in 3-D, an infected voxel may infect its six non-diagonal neighboring voxels with probabilities p_E , p_W, p_N, p_S, p_U and p_D where the probabilities are not necessary equal. Each region is grown until it reaches a certain volume since the number of voxels is a parameter in our model. The probability thresholds for each direction can be adjusted properly in order to obtain regions of a desired shape. Another extension to the original growth model is that we are modeling the degree of infection. Although in homogeneous regions all voxels are assigned the same value (or intensity), in non-homogeneous regions the value distribution of the voxels in the region follows the behavior of a usually monotonous decreasing function (with the number of epochs), simulating the intensity of a certain property for the internal area of the region. The voxel values in the second case can also be considered as probabilistic values for the presence of a property or inclusion of the voxel in the region of interest. Tumors or lesions in medical images are often considered to be homogeneous regions for simplicity although in most cases these are non-homogeneous regions with boundaries that are difficult to identify. Similarly, voxel values of statistical parametric maps of brain activation data denote the probability of that voxel being activated.

This model is also general enough to capture the possible anisotropy in growth due to surrounding tissue. Another

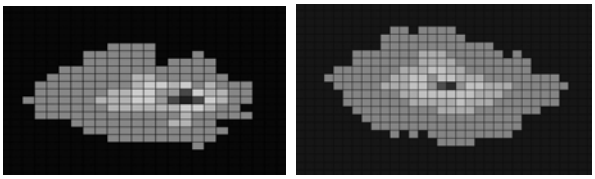

(a) (b)

Figure 3. Non-homogeneous regions elongated towards (a) one or (b) two opposite directions.

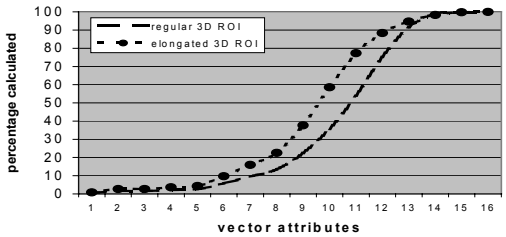

Figure 4. The feature vectors (f_r) of a spherical and an elongated 3D region.

extension to the original growth model is that we allow more than one initial cells to "infect" the space simultaneously. Each subregion has uniquely predefined parameters of growth (probability thresholds, centroid coordinates, and number of epochs). The region obtained as a combination of the subregions can reflect a higher variation of randomness. This makes the generation process more general in terms of being able to simulate complicated and more natural three-dimensional structures. One can use probability distributions collected from real data to model the number of initial points, their spatial location, the size of subregions, the direction of growth of each subregion in various stages, the depth of growth, the degree of infection, etc.

4. EXPERIMENTAL RESULTS

To verify the efficiency of the proposed characterization method, we experimented with both the process of obtaining the feature vector and the classification of given sets of region data in 3D and 2D. Here we present results for the 3D case. We also compare our proposed method to the one using morphological operators. In the experiments we used the Euclidean distance between the k-dimensional characterization vectors, obtained by our method, to classify the simulated regions. We used a radius increment step of 1 and k=15. In order to have a better comparative basis, we computed the morphological distances using the Euclidean norm (p=2) and sphere as the structural element. We used spherical homogeneous and elongated homogeneous and non-homogeneous regions. We considered 100 randomly generated images from each class of regions. The elongated regions were stretched to the north and south direction of growth. The non-homogeneous elongated regions were stretched either towards one of two opposite directions (see Figure 3). Each 3D volume consisted of 50×50×50 voxels. We implemented the methods in Matlab and run experiments on a single Pentium III Xeon processor workstation with 512 Mbytes of RAM running Linux. The experiments requiredmorphological istance calculations were carried out using the SDC Morphology Toolbox for MATLAB v1.1. The toolbox

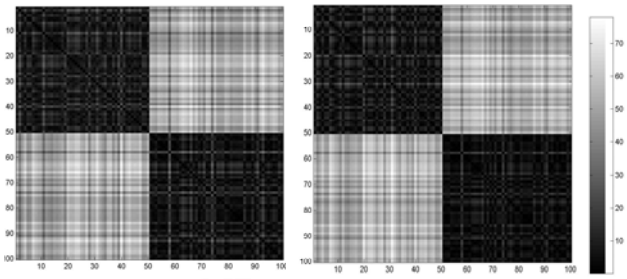

Figure 5. Euclidean distances of feature vectors f_r and f_s between all pairs of elongated and spherical 3D regions.

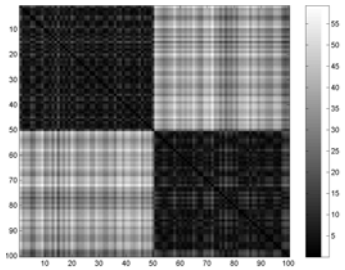

Figure 6. Euclidean distances of feature vectors f_r between all pairs of non-homogeneous elongated regions of type (a) and (b) of Figure 3.

provides implementations for both homogeneous and non-homogeneous (grey-scale) ROIs.

Figure 4 presents the variation of f_r features (signatures) for consecutive increments of the radius and for two types of 3D regions. Figure 5 shows the Euclidean distance values of the k-dimensional characterizing vectors for all pairs of homogeneous elongated and spherical regions and clearly identifies the existence of two distinct classes in the data set. In this case the f_s features are more discriminative than the f_r features.

In our next experiment we tested our proposed characterization technique on the problem of discriminating non-homogeneous regions elongated to both the north and south direction or to just one of the two (Figure 3 shows examples of the two types of regions). The resulting shapes are quite similar although their density concentration is in different subregions. Figure 6 demonstrates that the proposed method achieves impressive discriminative power. Experimentation with different increments of the radius for the concentric circles or spheres is in progress.

In order to compare the efficiency of our method to the one that uses the morphological distance we performed more classification experiments. Each morphological distance calculation between two 3D regions took approximately 11 minutes while the proposed method for characterization including the Euclidean distance calculation takes 7 seconds on the workstation we used. Due to the constraints imposed by the morphological distance calculations we performed the following experiments: (a) we picked one region from each class and calculated its distance to all the other regions and (b) we experimented with 2D regions instead of 3D. Here we report results from the first experiment. The structural element used in calculating the morphological distance was a disk (or a sphere in 3D) where M was equal to 20. Figures 7, 8 demonstrate that our method has performance comparable to, or even better (in non-homogeneous regions) than that of mathematical morphology.

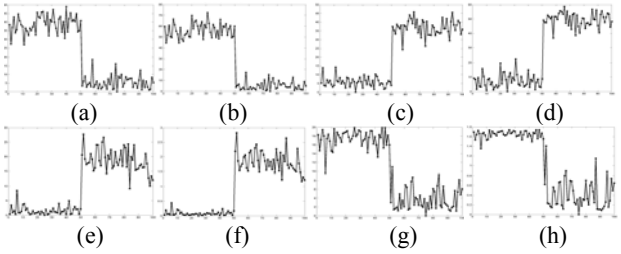

Figure 7. Euclidean distances of feature vectors between a spherical (a),(b) or an elongated (c),(d) homogeneous region and all other regions (using f_r (a),(c) and f_s (b),(d) features). (e),(f),(g), and (h) corresponding Euclidean distances for the two types of elongated non-homogeneous regions (stretched towards one and two opposite directions).

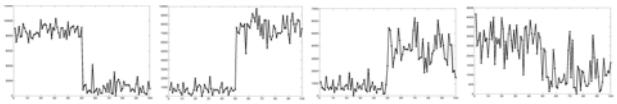

Figure 8. Morphological distances between a spherical (a) or an elongated (b) homogeneous region and all other regions. (c),(d) corresponding morphological distances for the two types of elongated non-homogeneous regions (stretched towards one and two opposite directions).

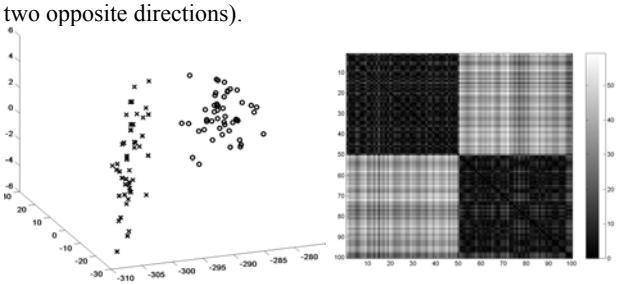

Figure 9. 3D scatter plot (a) of the 3 most significant attributes selected by SVD and the Euclidean distances (b) of the corresponding mapped data points of the two classes.

although it is two orders of magnitude faster. Applying SVD to reduce dimensionality to the 3 most significant transformed attributes improves the performance even further (Figure 9).

5. CONCLUSIONS AND FUTURE WORK

In this paper we presented a new method for fast and effective characterization of 3D (and 2D) homogeneous and non-homogeneous region data as well as a model for generating artificial region data. Work in progress includes the extension of the proposed characterization method so that it can be applied to non-homogeneous regions with more than one initial growing points.

6. ACKNOWLEDGEMENTS

This work was supported in part by National Science Foundation grant IIS-0083423.

7. REFERENCES

[1] A.W.M. Smeulders, M. Worring, S. Santint, A. Gupta, and R. Jain, "Content-Based Image Retrieval at the End of the Early Years," *IEEE Transactions on Pattern Analysis and Machine Intelligence*, vol. 22, pp. 1349-1380, 2000.

[2] A. Pentland, R. W. Picard, and S. Sclaroff, "Photobook: tools for content-based manipulation of image databases," in Proceedings of the *SPIE Conference, Storage and Retrieval of Image and Video Databases II*, San Jose, CA, 1994.

[3] M. Flickner, H. Sawhney, W. Niblack, J. Ashley, Q. Huang, b. Dom, and M. Gorkani, "Query by image and video content: the QBIC system," *IEEE Computer*, pp. 23-32, 1995.

[4] J. G. Dy, C. E. Brodley, A. C. Kak, C. Shyu, and L. S. Broderick, "The Customized-Queries Approach to CBIR," in Proceedings of the *IS&T/SPIE Electronic Imaging Conference: Storage and Retrieval for Image and Video Databases VII*, 1999.

[5] V. Megalooikonomou, J.Ford, L.Shen, F.Makedon, and A.Saykin, "Data mining in brain imaging", *Statistical Methods in Medical Research,* Vol. 9, No. 4, pp. 359-394, 2000.

[6] V. Megalooikonomou, D. Pokrajac, A. Lazarevic, Z. Obradovic, "Effective classification of 3-D image data using partitioning methods", to appear in Proceedings of the *SPIE 14th Annual Symposium in Electronic Imaging: Conference on Visualization and Data Analysis*, San Jose, CA, Jan. 2002.

[7] T. Pavlidis, "A review of algorithms for shape analysis," *Computer Graphics and Image Processing*, vol. 7, pp. 243-258, 1978.

[8] S. Loncaric, "A Survey of Shape Analysis Techniques," *Pattern Recognition*, vol. 31, pp. 983-1001, 1998.

[9] I.L. Dryden and K. V. Mardia, *Statistical Shape Analysis*: Wiley and Sons, 1998.

[10] P. Maragos, "Morphological skeleton representation and coding of binary images," *IEEE Transactions on Acoustics, Speech and Signal Processing*, vol. 34, pp. 1228-1244, 1986.

[11] F. Korn, N. Sidiropoulos, C. Faloutsos, E. Siegel, and Z. Protopapas, "Fast and effective retrieval of medical tumor shapes," *IEEE Transactions on Knowledge and Data Engineering*, vol. 10, pp. 889-904, 1998.

[12] J. Serra, *Image Analysis and Mathematical Morphology*. New York: Academic, 1982

[13] D. Sholl, "Dendritic Organization in the Neurons of the Visual and Motor Cortices of the Cat," J*ournal of Anatomy.*, vol. 87, pp. 387-406, 1953.

[14] M. Eden, "A two-dimensional growth process," in Proceedings of the *Fourth Berkeley Symposium on Mathematical Statistics and Probability,* Berkeley, CA, 1961.